Anomalous two-peak G # -band Raman effect in one isolated single-wall carbon nanotube

Anomalous two-peak G'-band Raman effect in one isolated single-wall carbon nanotube

A. G. Souza Filho,[1,2] A. Jorio,[1,3] A. K. Swan,[4] M. S. Ünlü,[4] B. B. Goldberg,[4] R. Saito,[5] J. H. Hafner,[6] C. M. Lieber,[6] M. A. Pimenta,[3] G. Dresselhaus,[7] and M. S. Dresselhaus[1,8]

[1]*Department of Physics, Massachusetts Institute of Technology, Cambridge, Massachusetts 02139-4307*

[2]*Departamento de Física, Universidade Federal do Ceará, Fortaleza-CE 60455-760, Brazil*

[3]*Departamento de Física, Universidade Federal de Minas Gerais, Belo Horizonte-MG, 30123-970 Brazil*

[4]*Electrical and Computer Engineering Department, and Department of Physics, Boston University, Boston, Massachusetts 02215*

[5]*Department of Electronic-Engineering, University of Electro-Communications, Tokyo 182-8585, Japan*

[6]*Department of Chemistry, Harvard University, Cambridge, Massachusetts 02138*

[7]*Francis Bitter Magnet Laboratory, Massachusetts Institute of Technology, Cambridge, Massachusetts 02139-4307*

[8]*Department of Electrical Engineering and Computer Science, Massachusetts Institute of Technology, Cambridge, Massachusetts 02139-4307*

(Received 23 May 2001; revised manuscript received 7 August 2001; published 8 February 2002)

The resonant second-order G'-band Raman spectra of *isolated* single-wall carbon nanotubes (SWNTs) exhibit an interesting resonance phenomenon, whereby the G' band for some special (n,m) isolated SWNTs exhibits a two-peak structure, while for most SWNTs, the G'-band profile is a single Lorentzian peak. The two-peak phenomenon is explained by combining the double-resonance Raman effect, originally introduced for graphite, with the singular electronic structure of SWNTs, which is unique for a given (n,m) pair. Therefore, the G'-band profile is strongly dependent on the joint density of electronic states and provides useful information about the electronic structure and on the (n,m) assignment for the specific SWNT that is in resonance with the laser.

DOI: 10.1103/PhysRevB.65.085417 PACS number(s): 73.22.−f

I. INTRODUCTION

The second-order G'-band frequency ($2500 < \omega_{G'} < 2900$ cm^{-1}) and its first-order related disorder-induced D-band frequency ($1250 < \omega_D < 1450$ cm^{-1}) in the Raman spectra of sp^2-bonded carbon materials have been known to exhibit a strongly dispersive behavior as a function of laser excitation energy ($1.0 < E_{\text{laser}} < 4.5$ eV).[1] Both the G' band and D band are associated with phonons close to the boundary (K point) of the Brillouin zone. Due to the momentum conservation constraint, the D band in sp^2 carbons exhibits significant Raman intensity only for *disordered* crystals[2] where the loss of translational symmetry allows the observation of phonons other than zone-center modes, which are not observed in perfect crystalline systems.[3] In contrast, the G' band is a second-order Raman feature that involves two phonons with wave vectors q and $-q$, thus automatically preserving the momentum conservation constraint. Therefore, the G' band is an intrinsic property of the two-dimensional (2D) graphene lattice and is present even in high-quality graphite crystals, where the D band is completely absent.[1] Study of the D band and G' band remains under active investigation, since its origin involves fundamental principles in the scattering of light by phonons.[4–15] The E_{laser}-dependent behavior of the ω_D and $\omega_{G'}$ phonon bands has been interpreted as due to a wave-vector-selective resonant process that relates k for electrons and q for phonons.[4–6,12] The physical origin for this phenomenon in graphite was recently explained by a double resonance process that involves the resonance of the incident/scattered photons with the interband transition (between valence π and conduction π^* bands) and, in addition, with an intermediate intraband scattering process mediated by a phonon.[8]

In single-wall carbon nanotube (SWNT) bundles, both the second-order G' band and its related first-order D band exhibit a dispersive behavior[9–11,13,14] for ω_D (or $\omega_{G'}$) vs E_{laser}, quite similar to graphite, but with intrinsic features that arise from the SWNT 1D electronic structure.[11,13,14] A steplike or oscillatory behavior appears[11,13,14] superimposed on the linear $\omega_{G'}$ vs E_{laser} behavior that is characteristic of graphite. This deviation in the dispersive behavior clearly shows the importance of considering the 1D electronic structure of SWNTs, which is uniquely determined for each (n,m) SWNT.[16] The singular 1D density of electronic states also allows the observation of the resonant Raman spectra from one isolated SWNT,[17] including both the G'-band and D-band features in the resonant Raman spectra.[18] The large dispersion of these bands provides a unique opportunity to observe new physical phenomena related to the Raman process itself, as will be illustrated in this paper, where the analysis of the G'-band spectra is carried out on individual SWNTs with known (n,m) indices.

In this paper we identify and study an interesting two-peak resonant Raman phenomenon in the G' band, which is observable only in isolated SWNTs. In the observation of the G'-band Raman spectra from isolated individual tubes, most of the spectra have Lorentzian shapes with one peak. However, in some special cases, we have observed *two peaks*. In this paper we show that the two possible G'-band profiles depend critically on the (n,m) values of the SWNTs and we explain this phenomenon in terms of a general double-resonance Raman effect introduced initially to account for the large dispersion of the G' band in graphite,[8] but adapted here to the singular joint density of states (JDOS) in SWNTs.[19] The double-resonance process together with the resonance with the SWNT JDOS (Ref. 19) give rise to the two different types of G'-band profiles. For certain (n,m)

SWNT indices, the double-resonance mechanism involves only a strong resonance with the incident photon, giving only one G'-band peak. However, there are a few special (n,m) SWNTs for which the electronic structure allows two different double-resonance processes to occur, one in connection with the incident photon and the other with the scattered photon. These two different double-resonance events are observed as two different frequencies in the G'-band Raman spectrum because of the large G'-band dispersion. Since the G'-band profiles are strongly dependent on the electronic structure of the resonant SWNT, we show how these G'-band spectra can then be used to obtain both electronic and structural information about SWNTs.

II. EXPERIMENTAL PROCEDURE

Isolated SWNTs were prepared by a chemical vapor deposition method on a Si substrate with a thin SiO_2 surface coating.[20] The sample used in this resonant Raman study has a very low SWNT density (less than 1 SWNT/μm^2) and a large diameter distribution, as measured by atomic force microscopy ($0.9 \leqslant d_t \leqslant 3.0$ nm). By scanning the sample in steps of 0.5 μm using a controlled microscope stage, isolated SWNTs within the E_{laser} resonant window ($2.31 \leqslant E_{\text{laser}} \leqslant 2.51$ eV) were found. Due to the low density of SWNTs per laser spot (spot size ≈ 1 μm diameter), the probability of finding one SWNT in the light spot that is in resonance with E_{laser} is less than 1/100. The spectral excitation was provided by an Ar-ion laser, using the 514.5 nm line ($E_{\text{laser}} = 2.41$ eV), with a power level $P < 10$ mW [power density ~ 1 MW/cm^2] at the sample surface. The scattered light was analyzed using a Renishaw 1000 B system equipped with a cooled charge-coupled device detector.

III. THEORETICAL BACKGROUND

The dispersion of the D band and G' band in graphite was recently explained by a double-resonance process,[8] where the Raman cross-section formula has two resonant factors in the denominator, which are both resonant at the same time, thereby giving a significant enhancement to the Raman D-band and G'-band intensities. The double resonance for graphite[8] always involves a resonant process for the intermediate state and involves also a second resonance when either the incident or scattered photon is resonant with an electronic π to π^* state transition. For a first-order scattering process as in the D band, the electrons have initial wave vectors k measured from the K point in the graphite Brillouin zone, and also a scattered electronic state with wave vector $k+q$ (q is the phonon wave vector), which satisfies the energy-momentum conservation relation

$$E(k+q) = E(k) \pm \hbar\omega_{\text{ph}}(q). \tag{1}$$

Here $\pm$ corresponds to a resonance process of the Stokes and anti-Stokes processes. Energy and momentum conservation requirements select two possible equi-energies $E(k+q)$ where the electrons have $k+q$ wave vectors (see Fig. 1). One of these equi-energies $E(k+q)$ exists around the same K point as the initial state k and the second is located around

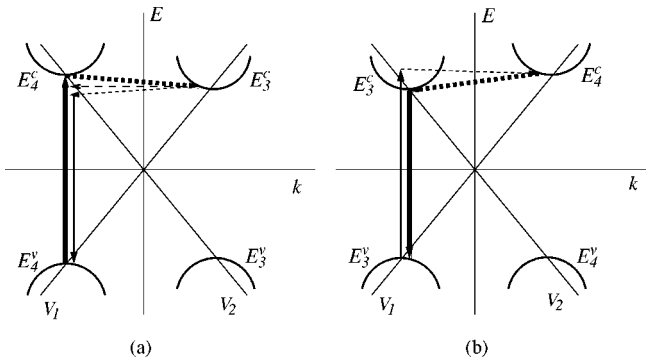

FIG. 1. Schematic diagram of the resonance Raman scattering processes contributing to the G'-band spectra in SWNT's adapted from Ref. 8. The boldface lines indicate the double-resonance process. In graphite, the double-resonance scattering occurs with two linearly dispersive bands with Fermi velocities V_1 and V_2 that cross the Fermi level at the K point in the graphite Brillouin zone and always involves the intermediate state (Ref. 8). For SWNT's, the linearly dispersive bands are replaced by confined states E_i ($i = 1,2,3,\ldots$) in the valence (E_i^v) and conduction (E_i^c) bands. Resonance Raman scattering involving the incident (a) or scattered (b) photons combined with intermediate states (see boldface lines) gives similar double-resonance processes as are described in Ref. 8. The long-dashed line in (a) denotes the double-resonance process for the D band described in Ref. 8 where the electron is inelastically scattered from one band to another by a phonon and then is scattered back elastically by an impurity or defect. This process is here adapted for the SWNT electronic structure. The short-dashed lines are for the inelastic process that is appropriate for the G' band.

the inequivalent K' point in the first Brillouin zone for graphite.[21] In the case of the first-order process, electrons in the state $k+q$ are elastically scattered by an impurity or defect to a final state with the wave vector k (see Fig. 1). For the G' band, which involves two phonons with q and $-q$ wave vectors, electrons in the $k+q$ states are now inelastically scattered to a final state with wave vector k (see Fig. 1). Of particular importance, the energy and momentum conservation requirements lead to a relation between the k for electrons and the q for phonons. By searching for a double resonance that satisfies the condition in Eq. (1) within the Brillouin zone of graphite, and by neglecting the trigonal warping effect for simplicity, we found that q values that satisfy the double-resonance condition[8] are preferentially located near $|q-q_0| \approx 2|k|$, where q_0 is the wave vector between K and K',[21] in agreement with the very recently published paper by Ferrari and Robertson.[15] It is expected that this factor of 2 will be modified slightly by the trigonal warping effect. We furthermore find that there is no simple analytic relation between q and k. The details of this calculation, including implications on the D-band and G'-band properties, is reported elsewhere.[21]

However, in the case of nanotubes, it is necessary to introduce some modifications into this model to account for the singular 1D electronic structure of SWNTs, for two reasons: (1) By rolling a graphene sheet into a small-diameter nanotube, the 2D structure collapses into a 1D structure due to the

boundary conditions along the nanotube circumference, which allow only certain quantized electronic states with selected k vectors to occur, and consequently the linear electronic dispersion relations $E(k)$ of graphite around the K point are reduced to a set of subbands; (2) the origin of the G' band in the Raman spectra for SWNT's is similar to that in graphite, but its observation is limited to having E_{laser} resonant with the van Hove singularities of the JDOS, which occur in the flat regions of the electronic dispersion curves $E(k)$ for the subbands.[16] Experimental evidence for the importance of these subbands in the D-band and G'-band properties comes from the step or oscillatory behavior observed in the frequency dispersion of the D and G' bands, ω_D and $\omega_{G'}$, vs E_{laser} for SWNT bundles.[11,13,14]

The Raman spectra for isolated SWNTs have measurable intensity only when the incident or scattered photon matches electronic transitions between subbands, such as the E_{33}^S and E_{44}^S transitions for semiconducting SWNTs that are frequently in resonance with $E_{\text{laser}}=2.41$ eV for our sample.[22] To account for the dispersive behavior of the phonon frequency vs E_{laser} observed in the D and G' bands for isolated SWNTs (Ref. 18) and for SWNT bundles,[9–11] it is necessary to consider also the double-resonance process in the context of SWNTs.[8] Moreover, since the van Hove singularity point in each conduction subband is a local energy minimum, the scattered electron states will in general lie in different energy subbands. Thus, we expect that the distribution of q vectors for each subband that is allowed by the double-resonance process will be in a much smaller range of q for SWNTs than for the case of graphite. This is one reason why the experimental results show a very small linewidth for the D band (down to 12 cm^{-1}) for SWNTs, when compared to graphite (30 cm^{-1}) (see Sec. IV). Two possible resonance processes for SWNTs are schematically described in Fig. 1, where we have adapted the double-resonance process in Ref. 8 to describe the double-resonance processes for the G' band subjected to the electronic structure in SWNTs. The processes illustrated by the horizontal long-dashed line in Fig. 1(a) give rise to the D-band spectra in SWNTs, and are similar to the processes occurring in graphite.[8] In the case of SWNTs, the process represented in Fig. 1(a) is appropriate in the present study for the incident photon in resonance with the E_{44}^S transitions and for a resonant intermediate state that involves an electron excited to the conduction subband E_4^c and is then scattered by a phonon to the conduction subband E_3^c. This process is indeed a double resonance process that gives rise to the G'-band dispersion in SWNTs, thus selecting a different phonon for each E_{ii}. Another possible resonant scattering process is described in Fig. 1(b), but in this case, one resonance comes from E_{44}^S through the intermediate state $(k+q)$, and the second resonance comes from the scattered photon that is resonant with the E_{33}^S transition. In the actual experiments presented here for specific (n,m) values, some photons follow the process in Fig. 1(a) and other photons follow the process in Fig. 1(b). Each incident and scattered photon contributes to its relevant peak in the G'-band profile, since different q vectors are selected for the E_{33}^S and E_{44}^S resonance scattering processes, and then $\Delta E_{ph1} \neq \Delta E_{ph2}$ because of the dispersion of $\omega_{G'}$ vs photon excitation energy.[11]

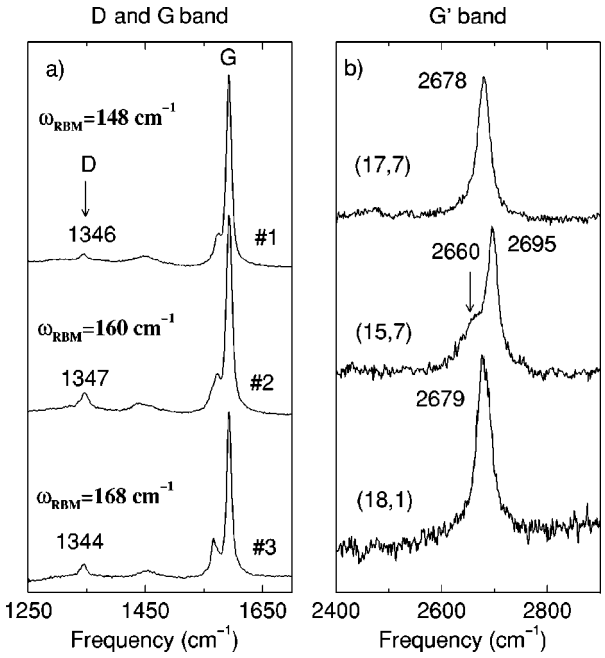

FIG. 2. Resonant Raman spectra of three different isolated SWNTs on a Si/SiO_2 substrate, using $E_{\text{laser}}=2.41$ eV (514.5 nm), showing the spectral range of the D and G band [Fig. 2(a)], and the second-order G' band [Fig. 2(b)]. The frequencies are displayed in units of cm^{-1}. The peak around 1450 cm^{-1} in Fig. 2(a) comes from the Si substrate. We also list the frequency of the radial breathing mode (ω_{RBM}) for each spectrum.

IV. RESULTS AND DISCUSSION

A. G'-band spectra in isolated tubes and (n,m) identification

Figure 2 shows three spectra for different isolated SWNTs obtained at different light spots on the sample. The features highlighted in Fig. 2 are the D band and G band [Fig. 2(a)], and the second-order G' band [Fig. 2(b)] where $\omega_{G'} \approx 2\omega_D$. We also list the frequency of the RBM (radial breathing mode) (ω_{RBM}) for each spectrum in Fig. 2. The (n,m) integers for the three spectra in Fig. 2 are identified by the RBM frequency analysis for isolated SWNTs ($\omega_{\text{RBM}} = 248/d_t$,[17] where d_t is the nanotube diameter in units of nanometers and $\gamma_0=2.89$ eV based on the Stokes/anti-Stokes intensity ratio studies on isolated semiconducting and metallic nanotubes[23,24]). The (n,m) assignment is further verified by the G'-band profile dependence on the van Hove singularities discussed below. Using this approach, the (n,m) indices of the isolated SWNTs in Fig. 2 are identified as: (17,7) for $\omega_{\text{RBM}}=148$ cm^{-1} (♯1), (15,7) for $\omega_{\text{RBM}}=160$ cm^{-1} (♯2), and (18,1) for $\omega_{\text{RBM}}=168$ cm^{-1} (♯3). All of the SWNTs in Fig. 2 are semiconducting, and the laser excitation ($E_{\text{laser}}=2.41$ eV) is resonant for observing ω_{RBM} with the E_{33}^S electronic transition for the (18,1) nanotube and with the E_{44}^S electronic transitions for the (17,7) and (15,7) nanotubes.

In the present paper, we measured the spectra for 24 physically different isolated semiconducting SWNTs where both the radial breathing mode and the second-order G' band were present. The (n,m) indices identification for each of the 24 SWNTs was carried out using the method given in Ref. 17. The related first-order D-band was either weak or absent in these spectra, thus indicating very good crystallinity of the SWNTs. Some of the SWNTs [see spectra ♯1 and ♯3 in Fig. 2(b)] show only one symmetric G' band Lorentzian peak, though some isolated SWNTs show two G' band peaks [see spectrum ♯2 in Fig. 2(b)]. The G'-band in 3D graphite also shows two peaks, but the physical origin of these two peaks is related to the coupling between the A and B graphene layers that are stacked in the highly ordered $\ldots ABAB \ldots$ structure.[3,6] The two-peak structure in the G'-band spectra for an *isolated* SWNT, where only one rolled graphene layer is present, cannot be explained in this way. The physical origin of the two G'-band peaks observed in the Raman spectrum of one isolated SWNT is a newly observed effect that can be understood by analyzing the resonance conditions related to the double-resonance process originally developed for graphite,[8] and by combining this process with a strongly resonant process connected with the JDOS of SWNTs.[19] We show in this paper that the resonant process associated with the JDOS for SWNTs makes the dominant contribution to the D- and G'-band Raman intensities.

By studying the D-band features for several *isolated* SWNTs, it was shown that both the G'-band and the D-band Raman signals[18] can be observed through resonance of either the *incident* or *scattered* photons with 1D van Hove singularities in the JDOS of SWNTs, and that the G'-band dispersive behavior is similar to that observed in SWNT bundles whose dispersion is given by $\bar{\omega}_{G'}(E_{\text{laser}}) = 2420 + 106\, E_{\text{laser}}$ (eV) in units of cm^{-1}.[11]

B. Two-peak Raman G'-band spectra

We show in Fig. 3 (left panels) two spectra where the G' band has two peaks whose differences in frequency between the two peaks are, respectively, 35 cm^{-1} and 28 cm^{-1} for the (15,7) and (13,11) nanotubes, where the indicated (n,m) values have been identified by the method previously reported.[17] In the upper right panel the JDOS is shown for the (15,7) SWNT. The energy of the incident photons ($E_{\text{laser}} = 2.41$ eV) and scattered photons ($E_{\text{laser}} - E_{G'} \approx 2.41 - 0.33 = 2.08$ eV) are plotted as vertical dashed lines and the horizontal double arrows indicate the energy ranges where the resonance with the incident and the scattered photons can be observed.[17] By taking the difference in energy between the two components of the G' band (35 and 28 cm^{-1}) and the slope 106 cm^{-1}/eV for the dispersion in SWNT bundles,[11] we obtain 0.30 and 0.26 eV, and these values are close to the phonon energy $E_{G'} \approx 0.33$ eV observed with $E_{\text{laser}} = 2.41$ eV. A similar analysis can be carried out for the (13,11) SWNT plotted in the lower right panel. By analyzing the G'-band profile of the lower left spectrum of Fig. 3, we see that the intensity ratio between the upper frequency component to the lower frequency component is larger for the (13,11) SWNT than for the (15,7) SWNT, in accordance with the prediction (shown in the right panels), that the incident photon for the (13,11) SWNT is closer to the E_{44}^S singularity than the scattered photon is to E_{33}^S. For the (15,7) nanotube, the more nearly equal energy differences $(E_{44}^S - E_{\text{laser}})$ and $[E_{33}^S - (E_{\text{laser}} - E_{G'})]$ lead to a larger value for the Raman intensity ratio of the lower frequency component to the higher frequency component of the G' band. The analysis presented here is valid when all Raman features come from the same isolated SWNT, as is the case in the present experiment. From the analysis outlined in Fig. 3, we conclude that the lower and upper components in the G'-band spectra for isolated SWNTs come from two different double resonance processes, one involving the scattered photon [Fig. 1(b)], the other involving the incident photon [Fig. 1(a)], and each of the two photons is resonant with *different* E_{ii} singularities in the JDOS. It should be pointed out that different electron-hole pairs are involved in each process sketched in Fig. 1, but that the resonance denominators in the Raman cross section are the same.

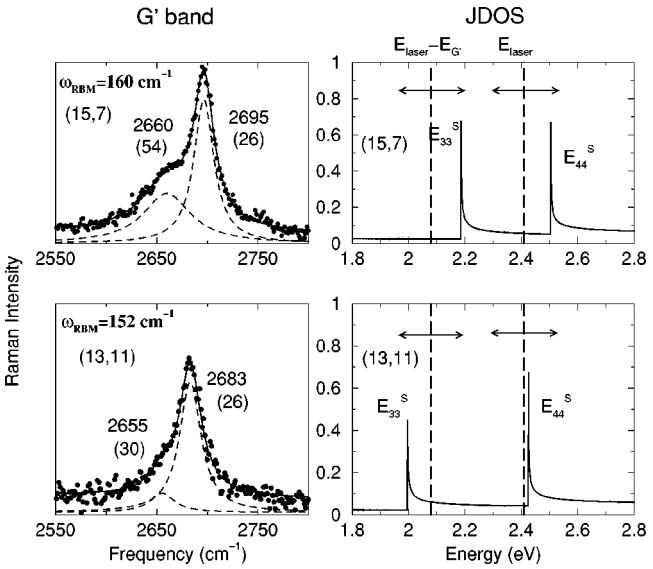

FIG. 3. G'-band profile (left panel) and joint density of electronic states (right panel) for the (15,7) and (13,11) SWNTs. Each G'-band profile has two peaks indicating that a double resonance process is occurring with both the incident and scattered photons, as depicted in the joint density of states (right panel). The E_{laser} energy is resonant with E_{44}^S for the (15,7) and (13,11) SWNTs, respectively, and the scattered photon is resonant with E_{33}^S, as schematically represented in Figs. 1(a) and 1(b). The vertical dashed lines represent $E_{\text{laser}} = 2.41$ eV and $E_{\text{laser}} - E_{G'} \approx 2.08$ eV. The horizontal double arrows stand for the energy range where the resonance can be observed, also called the resonant window. The G'-band frequencies (linewidths) are in units of cm^{-1}.

By considering the diameter distribution of the isolated SWNTs dispersed on the Si/SiO_2 substrate and the energy of the laser line ($E_{\text{laser}} = 2.41$ eV), we can theoretically predict the (n,m) values that will exhibit *two peaks* in the G'-band spectra and those SWNTs that will exhibit only one G'-band peak, including the E_{ii} transitions that are involved in the resonance. Among the eight tubes predicted to exhibit two

TABLE I. Assigned (n,m) indices, diameters d_t, the E_{22}^S, E_{33}^S, and E_{44}^S electronic transitions, the RBM, D-band, and G'-band frequencies for the isolated SWNTs predicted to be resonant with $E_{\text{laser}}=2.41$ eV. The tubes for which the E_{44}^S transition is resonant with $E_{\text{laser}}=2.41$ eV are divided into two groups, namely, the tubes whose G' band has two peaks (double resonance involving the incident and scattered photons) and one peak (double resonance involving only the incident photon). The singularities in boldface and italics indicate a resonance with the incident and scattered photons, respectively. The numbers between brackets and parentheses, respectively, stand for the number of times a particular (n,m) SWNT was observed in the experiment and the linewidths for the D-band and G'-band features. The theoretical values used for the RBM frequency are $\omega_{\text{RBM}}=248/d_t$ ($a_{\text{C-C}}=0.144$ nm) and $\gamma_0=2.89$ eV based on Refs. 16, 23, and 24.

(n,m)	d_t (nm)	E_{22}^S (eV)	E_{33}^S (eV)	E_{44}^S (eV)	ω_{RBM} (cm^{-1}) Theory	Exp.	D band (cm^{-1})	G' band (cm^{-1})	
			Nanotubes in resonance with E_{44}^S					(Two peaks)	
(16,8)	1.68	0.97	*2.00*	**2.34**	147.6				
(15,7)	1.54	1.05	*2.18*	**2.50**	160.5	160[2]	1347(17)	2660(54)	2695(26)
(13,11)	1.65	0.99	*1.99*	**2.43**	150.1	152[2]	—	2655(30)	2683(26)
(17,6)	1.64	0.98	*2.08*	**2.37**	151.2				
(14,9)	1.59	1.02	*2.09*	**2.47**	155.6				
(18,4)	1.61	1.01	*2.14*	**2.39**	153.9	154[2]	1347(33) [a]	2665(35)	2690(29)
(20,0)	1.59	1.01	*2.20*	**2.40**	156.2				
(19,2)	1.59	1.01	*2.19*	**2.40**	155.6	155[4]	1348(16)	2665(47)	2689(27)
								(One peak)	
(22,3)	1.88	0.90	1.67	**2.33**	132.1				
(23,1)	1.87	0.91	1.68	**2.36**	132.8				
(18,8)	1.83	0.92	1.73	**2.32**	135.4				
(19,6)	1.79	0.94	1.76	**2.39**	138.2	139[1]	1341(20)	2679 (30)	
(20,4)	1.77	0.96	1.77	**2.47**	140.3				
(16,9)	1.74	0.96	1.83	**2.41**	142.4				
(13,12)	1.72	0.96	1.89	**2.37**	144.2	144[1]	1342(17)	2680(28)	
(17,7)	1.70	0.99	1.86	**2.50**	146.1	148[3]	1346(15)	2678(28)	
(14,10)	1.66	1.00	1.93	**2.49**	149.6	150[4]	1343(15) [b]	2682(26)	
			Nanotubes in resonance with E_{33}^S					(One peak)	
(17,3)	1.48	1.08	**2.36**	2.55	167.2				
(18,1)	1.47	1.09	**2.39**	2.56	168.7	168[1]	1344(14)	2679(33)	
(14,6)	1.41	1.14	**2.41**	2.71	175.7	175[1]	1346(13)	2683(37)	
(11,9)	1.38	1.19	**2.38**	2.85	180.1	181[1]	—	2680(32)	
(15,4)	1.38	1.16	**2.51**	2.74	180.1	180[1]	1347(12)	2685(30)	
(13,6)	1.34	1.26	**2.34**	3.13	185.7				
(10,9)	1.31	1.27	**2.46**	3.04	189.8				
(14,4)	1.29	1.31	**2.38**	3.31	190.8				
(15,2)	1.28	1.30	**2.40**	3.46	194.1	193[1]	1346(30)	2682(34)	
(16,0)	1.27	1.35	**2.40**	3.52	195.2				

[a]The D-band intensity is very weak. Only one of the two (18,4) tubes showed any D-band intensity.
[b]Among the four (14,10) tubes that were observed, one of them did not show any D-band intensity.

peaks in the G' band for $E_{\text{laser}}=2.41$ eV (see Table I), we have so far observed four of them, and they are also listed in Table I. For these tubes, the E_{laser} is resonant with the E_{44}^S electronic transition and $E_{\text{laser}}-E_{G'}$ is resonant with the E_{33} transition. For some (n,m) values, Raman spectra from more than one physical nanotube were observed at different spots on the sample. Also, the Raman spectra from different SWNTs with the same (n,m) values showed the same spectral characteristics, namely, the same frequencies and the same relative intensities for all the Raman features, except for the D-band intensity. This allowed us to obtain more accurate values for the frequencies and linewidths for the G'-band peaks (see Table I).

C. One-peak Raman G'-band spectra

We now consider the situation where the G' band has only one peak, as occurs for most of the (n,m) SWNTs that were measured in the present paper. The first example we show is for the (19,6) SWNT, which is resonant with E_{44}^S, and here the G'-band does not exhibit a two-peak structure (see upper left panel in Fig. 4), thus indicating that the double-resonance process involves only one E_{ii} transition, and this is the one that is in resonance with the incident photon energy E_{laser} [process shown in Fig. 1(a)]. The double resonance involving the scattered photon is not favorable since $E_{\text{laser}}-E_{G'}$ is far from the E_{33}^S transition, as observed in the JDOS plot for this tube shown in the upper right panel

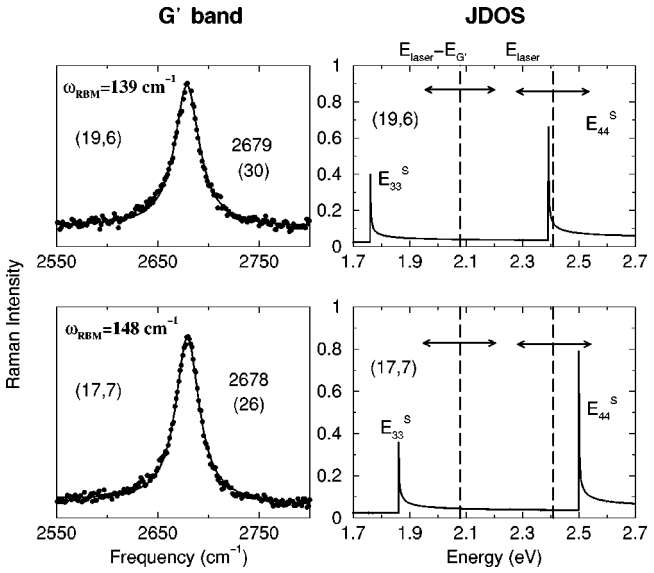

FIG. 4. G'-band profile (left panel) and joint density of electronic states (right panel) for the (19,6) and (17,7) SWNTs. Each G'-band profile has only one peak, indicating that the resonance is only with the incident photon. The E_{laser} energy is resonant with E_{44}^S for the (17,7) and (19,6) SWNTs. The vertical dashed lines represent $E_{\text{laser}}=2.41$ eV and $E_{\text{laser}}-E_{G'}\approx 2.08$ eV. The horizontal double arrows stand for the energy range where the resonance can be observed, also called the resonant window. The G'-band frequencies (linewidths) are in units of cm^{-1}.

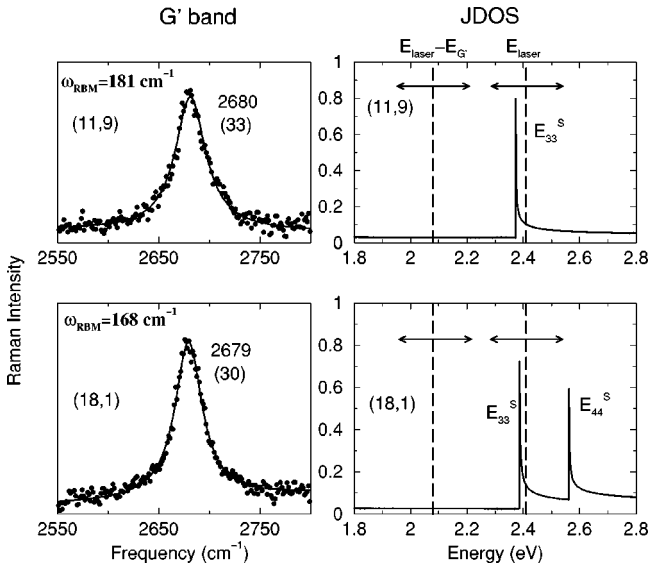

FIG. 5. G'-band profile (left panel) and joint density of electronic states (right panel) for the (11,9) and (18,1) SWNTs. Each G'-band profile has only one peak, indicating that the double resonance involves only the incident photon. The E_{laser} energy is resonant with E_{33}^S for both the (11,9) and (18,1) SWNTs. The vertical dashed lines represent $E_{\text{laser}}=2.41$ eV and $E_{\text{laser}}-E_{G'}\approx 2.08$ eV. The horizontal double arrows stand for the energy range where the resonance can be observed, also called the resonant window. The G'-band frequencies (linewidths) are in units of cm^{-1}.

of Fig. 4. Nine (n,m) nanotubes, where E_{laser} is resonant with E_{44}^S, were predicted (see Table I) to have a G' band with only one peak. We have experimentally observed four of these nine tubes and only one peak in the G'-band spectra was indeed found for these (n,m) tubes. No tubes other than those listed in Table I were found to be in resonance with E_{44}^S and to have only one G'-band peak.

The consistency between the observed and predicted G'-band profiles makes it possible to use our model to verify the (n,m) assignment given by the RBM properties and to give further evidence for the use of resonance Raman spectroscopy to yield (n,m) structural information. This is illustrated by the case for the SWNT with $\omega_{\text{RBM}}=148$ cm^{-1}, which is resonant with E_{44}^S. Here the G' band does not exhibit the *two-peak* structure (see lower left panel in Fig. 4), thus indicating that the resonance is only with the incident photon. The resonance cannot in this case be only with the scattered photon, since the RBM feature is also observed. From the relation $\omega_{\text{RBM}}=248/d_t$, there are two likely (n,m) candidates for $\omega_{\text{RBM}}=148$ cm^{-1}, namely, (16,8) and (17,7). Since the G' band shows only a single symmetric Lorentzian peak, this nanotube is identified with (17,7), where only the double resonance involving the incident photon (E_{laser}) occurs with the E_{44}^S transition. The double-resonance process involving the scattered photon is not favorable in this case since $E_{\text{laser}}-E_{G'}$ is far from the E_{33}^S transition, as observed in the JDOS plot for this tube shown in the lower right panel of Fig. 4. On the other hand, the energies of the E_{33}^S and E_{44}^S transitions for the (16,8) nanotube are 2.00 and 2.34 eV, respectively, which implies that the scattered photon ($E_{\text{laser}}-E_{G'}=2.08$ eV) would be close enough to the E_{33}^S transition to result in a G'-band profile with two peaks, which is not observed experimentally, so that we can eliminate the (16,8) assignment for this tube.

The last category considered in Table I is illustrated in Fig. 5 for SWNTs with $\omega_{\text{RBM}}=181$ and 168 cm^{-1}, for which E_{laser} is resonant with E_{33}^S, and the G' band has also only one peak (see upper and lower left panels in Fig. 5) where their (n,m) are assigned as (11,9) and (18,1), respectively. Here, E_{laser} is resonant with E_{33}^S and only one peak is expected in the G' band, since for all the observable nanotubes within the diameter range of our sample, the E_{22}^S transition is far from E_{33}^S. For these particular SWNTs, only one double-resonance process involving the incident photon [see Fig. 1(a)] is observable. Following the predictions summarized in Table I, all (n,m) tubes for which E_{laser} is resonant with E_{33}^S are listed, and for all of these tubes, the G' band should have only one peak. Among the ten tubes predicted to be in resonance with E_{33}^S (see Table I), five of these tubes were observed experimentally and all were found to exhibit only one G'-band peak.

D. Isolated SWNTs vs SWNT bundles

Finally, to recover the G'-band spectra for SWNT bundles based on the spectroscopy for isolated tubes, we can analyze our current G'-band frequencies for isolated SWNTs listed in Table I. In this table, we do not list the spectra for which we observed resonance only with the scattered photon,

since in this case the RBM would not be observed and a complete (n,m) assignment for the SWNT would then not be possible. Measurements that we made on 16 different (n,m) isolated SWNTs in the sample that were resonant with E_{44}^S and E_{33}^S show that the upper (lower) component of their G'-band profile has a frequency that is a little higher (lower) than $\bar{\omega}_{G'}$ reported for SWNT bundles (where $\bar{\omega}_{G'}$ is used to denote the G'-band peak frequency for the SWNT bundles).[11] We attribute this frequency difference to the fact that in SWNT bundles, the G'-band profiles include double resonances involving either the incident or the scattered photons for many different SWNTs (and in a few cases double resonances involving the incident and scattered photons are observed as illustrated in this paper), thus resulting in an average phonon G'-band frequency. By using $E_{\text{laser}}=2.41$ eV, the G'-band frequencies in SWNT bundles have been reported to be 2676 cm^{-1},[9] 2670 cm^{-1},[10] and 2670 cm^{-1}.[11] The average between the upper and lower G'-band components for the isolated SWNTs listed in Table I is 2672 cm^{-1}, in excellent agreement with the results for SWNT bundles reported in Refs. 9–11. As expected, the linewidths for both the D band and the upper component of the G' band for isolated SWNTs appear to be much narrower (see Table I) than for SWNT bundles, where both the D band and G' band show linewidths of about 60 cm^{-1}.[9,11,13] The larger linewidths in the bundles are associated with different resonant frequencies for different nanotubes within the bundles and contributions from resonances with the incident photon for some tubes and with the scattered photon for other tubes. The frequencies of the G' band seem to exhibit a dependence on the energy difference between E_{laser} and the energy of the singularities E_{ii} (i.e., $|E_{\text{laser}}-E_{ii}|$), which is reasonable, based on the dispersive origin of the G' band. A detailed calculation of the Raman cross section for the resonant process in SWNTs would require taking into account the detailed energy dispersion of each of the SWNT subbands involved in the resonant transitions, and such a calculation will be reported elsewhere.

V. CONCLUSIONS

In summary, we report here a study of the characteristics of the second-order G' band for isolated, semiconducting SWNTs. In some spectra a *two-peak* structure is observed in the G'-band feature for isolated SWNTs, arising in special cases where the double-resonance process (originally proposed for graphite[8]) involves the incident photon with one electronic transition or the scattered photon with another electronic transition. Each peak in the G' band thus arises from the resonance with different singularities in the joint 1D density of electronic states (JDOS), involving a different electron-hole pair for each process. This phenomenon is explained by considering the G'-band dispersion (which comes from a double-resonance process in graphite[8]) along with the 1D JDOS that defines the special interband transitions between van Hove singularities in SWNTs. In most cases only one peak is observed in the G' band, consistent with our model. The model presented here describes qualitatively the observed phenomena, taking into account only the most important resonant contributions that come from the JDOS. A detailed analysis should be performed, considering the very complicated electronic and phonon dispersion processes that occur for individual (n,m) SWNTs. We show that this newly observed effect for the G' band reveals detailed information about the electronic structure of the SWNTs. The information provided in Table I can also be useful for verifying (n,m) assignments that were made for isolated SWNTs, using resonance Raman scattering as an (n,m) characterization method.[17] The spectra from the isolated tubes can also explain some properties of the corresponding G'-band spectra previously reported for SWNT bundles.[9–11]

ACKNOWLEDGMENTS

A.G.S.F. and A.J. acknowledge financial support from the Brazilian agencies CAPES and CNPq, respectively. A.K.S. and B.B.G. acknowledge support from Renishaw Inc. The experimental work was performed at Boston University at the Photonics Center, operated in conjunction with the Department of Physics and the Department of Electrical and Computer Engineering. R.S. acknowledges a Grant-in-Aid (No. 13440091) from the Ministry of Education, Japan. The MIT authors acknowledge support under NSF Grants Nos. DMR 01-16042, INT 98-15744, and INT 00-00408.

[1] R. P. Vidano, D. B. Fishbach, L. J. Willis, and T. M. Loehr, Solid State Commun. **39**, 341 (1981).
[2] F. Tuinstra and J. L. Koenig, J. Chem. Phys. **53**, 1126 (1970).
[3] M. S. Dresselhaus and G. Dresselhaus, in *Light Scattering in Solids III*, edited by M. Cardona (Springer, Berlin, 1982), Chap. 2.
[4] I. Pócsik, M. Hundhausen, M. Koós, and L. Ley, J. Non-Cryst. Solids **227-230**, 1083 (1998).
[5] M. J. Matthews, M. A. Pimenta, G. Dresselhaus, M. S. Dresselhaus, and M. Endo, Phys. Rev. B **59**, 6585 (1999).
[6] A. C. Ferrari and J. Robertson, Phys. Rev. B **61**, 14 095 (2000).
[7] P. H. Tan, Y. Tang, C. Y. Hu, F. Li, Y. L. Wei, and H. M. Cheng, Phys. Rev. B **62**, 5186 (2000).
[8] C. Thomsen and S. Reich, Phys. Rev. Lett. **85**, 5214 (2000).
[9] S. D. M. Brown, P. Corio, A. Marucci, M. A. Pimenta, M. S. Dresselhaus, and G. Dresselhaus, Phys. Rev. B **61**, 7734 (2000).
[10] C. Thomsen, Phys. Rev. B **61**, 4542 (2000).
[11] M. A. Pimenta, E. B. Hanlon, A. Marucci, P. Corio, S. D. M. Brown, S. A. Empedocles, M. G. Bawendi, G. Dresselhaus, and M. S. Dresselhaus, Braz. J. Phys. **30**, 423 (2000).
[12] C. Castiglioni, C. Mapelli, F. Negri, and G. Zerbi, J. Chem. Phys. **114**, 963 (2001).
[13] S. D. M. Brown, A. Jorio, G. Dresselhaus, and M. S. Dresselhaus, Phys. Rev. B **64**, 073403 (2001).
[14] A. Grüneis, M. Hulman, Ch. Kramberger, T. Pichler, H. Peterik, H. Kuzmany, H. Kataura, and Y. Achiba, in *Proceedings of the*

International Winter School on Electronic Properties of Novel Materials—2001, edited by H. Kuzmany, M. Mehring, and J. Fink, AIP Conf. Proc. No. **591** (American Institute of Physics, Melville, N.Y., 2002), p. 319.

[15] A. C. Ferrari and J. Robertson, Phys. Rev. B **64**, 075414 (2001).

[16] R. Saito, G. Dresselhaus, and M. S. Dresselhaus, in *Physical Properties of Carbon Nanotubes* (Imperial College Press, London, 1998).

[17] A. Jorio, R. Saito, J. H. Hafner, C. M. Lieber, M. Hunter, T. McClure, G. Dresselhaus, and M. S. Dresselhaus, Phys. Rev. Lett. **86**, 1118 (2001).

[18] M. A. Pimenta, A. Jorio, S. D. M. Brown, A. G. Souza Filho, G. Dresselhaus, J. H. Hafner, C. M. Lieber, R. Saito, and M. S. Dresselhaus, Phys. Rev. B **64**, 041401R (2001).

[19] The joint density of electronic states (JDOS) is given by $\mathrm{JDOS}(\hbar\omega) = (1/4\pi^3)\int \delta[E_i^c(k) - E_i^v(k) - \hbar\omega]dk$, where E_i^c and E_i^v are the energies for the ith electronic state in the conduction (c) and valence (v) bands, respectively.

[20] J. H. Hafner, C. L. Cheung, T. H. Oosterkamp, and C. M. Lieber, J. Phys. Chem. B **105**, 743 (2001).

[21] R. Saito, A. Jorio, A. G. Souza Filho, G. Dresselhaus, M. S. Dresselhaus, and M. A. Pimenta, Phys. Rev. Lett. **88**, 027401 (2002).

[22] M. S. Dresselhaus and P. C. Eklund, Adv. Phys. **49**, 705 (2000).

[23] A. G. Souza Filho, A. Jorio, J. H. Hafner, C. M. Lieber, R. Saito, M. A. Pimenta, G. Dresselhaus, and M. S. Dresselhaus, Phys. Rev. B **63**, 241404R (2001).

[24] Z. Yu and L. E. Brus, J. Phys. Chem. B **105**, 6381 (2001).